Published as:
Belali, S.; Emandi, G.; Cafolla, A. A.; O'Connell, B.; Haffner, B.; Möbius, M. E.; Karimi, A.; Senge, M. O. (2017):
Water-soluble, neutral 3,5-diformyl-BODIPY with extended fluorescence lifetime in a self-healable chitosan hydrogel.
Photochemical & Photobiological Sciences 16, 1700–1708. doi: 10.1039/C7PP00316A

Journal Name

ARTICLE

Water-soluble, neutral 3,5-diformyl-BODIPY with extended fluorescence lifetime in a self-healable chitosan hydrogel

Received 00th January 20xx,
Accepted 00th January 20xx

DOI: 10.1039/x0xx00000x

www.rsc.org/

Simin Belali,[a,b] Ganapathi Emandi,[a] Atillio A. Cafolla,[c] Barry O'Connell,[d] Benjamin Haffner,[e] Matthias E. Möbius,[e] Alireza Karimi[b] and Mathias O Senge*[a]

3,5-Diformyl-4,4-difluoro-4-bora-3a,4a-diaza-*s*-indacene (3,5-diformyl-BODIPY) can be used as an efficient biofunctional cross-linker to generate a new class of chitosan-based hydrogels with fluorescence resonance energy transfer (FRET) dynamics and good solubility in water. The hydrogel was fully characterized by FT-IR, UV-vis, fluorescence, FE-SEM, AFM, rheology and picosecond time-resolved spectroscopic techniques. The self-healing ability was demonstrated by rheological recovery and macroscopic and microscopic observations. The fluorescence lifetime was found that increased in aqueous solution of the BODIPY-chitosan hydrogel compared to the 3,5-diformyl-BODIPY monomer. Calculations based on experimental results such as red-shift and decreased intensity of the emission spectrum of highly dye-concentrated hydrogel in comparison to dilute hydrogels, together with changes in the fluorescence lifetime of the hydrogel at different concentration of dyes, suggest that the BDP-CS hydrogel's fluorescence dynamics obey the Förster resonance energy transfer (FRET). Improvements in mechanical and photochemical properties and the acceptable values of BODIPY fluorescence lifetime in the hydrogel matrix indicate the utility of the newly synthesized hydrogels for biomedical applications.

Introduction

4,4-Difluoro-4-bora-3a,4a-diaza-*s*-indacene (BODIPY) dyes have special properties such as large molar extinction coefficients, sharp emission and high fluorescence quantum yield.[1] These attributes have elicited wide interest in applications of these dyes as imaging agents and many other areas.[2] However, some of these fluorescence probes show undesirable properties such as poor compatibility with living cells, instability or toxicity, which restricts their practical use.[3] In addition, their low water solubility causes aggregation through π–π-stacking interactions, which significantly reduces their fluorescence quantum yield and subsequently hinders use in biological media.[4] Most reported strategies to make these dyes water-soluble generally include introduction of ionic hydrophilic groups such as carboxylic or sulfonic acids or ammonium groups.[5] Neutral, water soluble BODIPY dyes have advantages over ionic ones as they avoid potential nonspecific interactions between BODIPY dyes and biomolecules in biomedical applications.[6a] Although introduction of oligo(ethyleneglycol) chains, α-galactosylceramide, peptides, or polymers improves water solubility, the absence of aggregation and strong fluorescence were only observed with less conjugated dyes, i.e. those with a low concentration of BODIPY units.[6] Thus, it is necessary to develop general approaches to significantly enhance the water-solubility of BODIPY dyes whereby the formation of non-fluorescent dimers and higher aggregates is prevented. We suggest that incorporation of BODIPY dyes into a hydrogel network as a cross-linker could effectively increase the solubility of BODIPY dyes and significantly reduce their aggregation via π–π-interactions and enhance their fluorescence quantum yields.

Hydrogels are currently attracting interest in biomedical applications due to their high water contact capacity and low interfacial tension with the surrounding area.[7] Use of a hydrogel network with a hydrophilic structure as host could effectively enhance enthalpic interactions of BODIPY dye molecules with water and significantly increase its water solubility, and also reduce their aggregation.[8] BODIPY have been incorporated into hydrogels before; however, mostly as simple inclusion compounds.[9] Examples for covalent bonding[6a] include coupling via peptide sequences or azide click reactions to PEG hydrogels.[10]

Different natural polymers have been used as structural materials in hydrogels, due to their intrinsic biocompatibility,

[a] *School of Chemistry, SFI Tetrapyrrole Laboratory, School of Chemistry, Trinity Biomedical Sciences Institute, Trinity College Dublin, The University of Dublin, 152-160 Pearse Street, Dublin 2, Ireland*
[b] *Department of Chemistry, Faculty of Science, Arak University, Arak 38156-8-8349, Iran*
[c] *School of Physical Sciences, Dublin City University, Glasnevin, Dublin 9, Ireland*
[d] *Nano Research Facility, Dublin City University, Glasnevin, Dublin 9, Ireland*
[e] *Sami Nasr Institute of Advanced Materials (SNIAM), School of Physics, Trinity College Dublin, The University of Dublin, Dublin 2, Ireland*

† Electronic Supplementary Information (ESI) ^{1}H NMR, ^{13}C NMR, ^{19}F NMR, and ^{11}B NMR spectrum of 3,5-diformyl-4,4-difluoro-4-bora-3a,4a-diaza-s-indacene in $CDCl_3$. FE-SEM images of nanofiber BDP-CS hydrogel structure and pore size distributions of the hydrogels with different wt-% 3,5-diformyl BODIPY as a cross-linker. Stability of hydrogel at different pHs, normalized emission spectra of BDP-CS hydrogel at different concentrations. See DOI: 10.1039/x0xx00000x

low toxicity and susceptibility to enzymatic degradation.[7,11] Chitosan is one of these attractive polysaccharides, which also does not induce an immune response.[12] These properties make it a very versatile material for many applications in the biomedical and biotechnological areas. Chitosan (CS) is a linear polysaccharide composed of randomly distributed β-(1-4)-linked D-glucosamine and *N*-acetyl-D-glucosamine units. Chitosan based hydrogels have been prepared with a variety of cross-linkers as liquid gels, films, sponges, and more.[13]

Here we chose 3,5-diformyl-BODIPY (BDP) as a cross-linker using a rapid, dynamic Schiff-base reaction between chitosan with amine functional groups and the aldehyde groups of 3,5-diformyl-BODIPY (Figure 2c,d). The BODIPY–cross-linked hydrogels are stable, injectable and self-healable which facilitates long-term fluorescent properties with potential for *in vivo* applications. As the BODIPYs are not physically conjugated, there is no migration out of the hydrogel networks. The formation of a 3D-network gives a high, homogeneous spatial density of BODIPY. This prevents BODIPY aggregation and fluorescence self-quenching, which can occur during BODIPY conjugation to polymers in aqueous solution. Additionally this injectable, self-healing BODIPY hydrogel, could potentially reassemble as an integral hydrogel, without the risk of premature polymerization, for *in vivo* applications such as an implantable hydrogel for fluorescence imaging.[14]

Experimental

Materials

Medium molecular weight of chitosan (190,000-310,000 Da), 75-85% deacetylated and viscosity 200-800 128 cP, 1 wt-% in 1 % acetic acid was obtained from Sigma-Aldrich. All solvents and reagents were purchased from Sigma-Aldrich and were used without any purification. Deionized and distilled water were used for all aqueous solutions. 3,5-Diformyl-4,4-difluoro-4-bora-3a,4a-diaza-*s*-indacene was prepared as described in the literature.[15]

Preparation of covalently cross-linked BDP-CS hydrogels

A 3 % (w/v) chitosan solution was prepared by dissolving chitosan (15 mg) in (1 % (v/v)) aqueous acetic acid. The mixture was stirred at 30 °C for 15 min to assure that all chitosan was completely dissolved. This was combined in variable weight proportions with a solution of 3,5-diformyl-BODIPY to give the required mass ratios of BODIPY-chitosan. For the preparation of BDP-CS hydrogels a solution of BDP as cross-linker was prepared by dissolving 4.5 mg BDP in 4 mL of aqueous DMF (0.013 M). For different hydrogels, the amount of 3,5-diformyl-BODIPY was varied from 12 to 4.5 mg. The BDP solution was added to the chitosan solution and the blend was mixed. Gelation occurred within 2 h. Finally, the hydrogels were immersed in distilled water for 12 h to remove DMF and unreacted chemicals. Residual DMF was removed under reduced pressure.

Spectroscopy

^{1}H NMR spectra were recorded on Bruker Advance III 400 MHz, Bruker DPX400 400 MHz, or an Agilent 400 spectrometer in $CDCl_3$. UV-vis absorption measurements were performed with a Specord 250 spectrophotometer. Fluorescence emission spectra were obtained using a Varian Cary-Eclipse instrument. Infrared spectra were recorded on a Mattson Genesis II FTIR spectrophotometer equipped with a Gateway 2000 4DX2-66 workstation. The fluorescence quantum yields (Φ_f) were estimated from the emission and absorption spectra by a comparative method at an excitation wavelength of 488 nm using Rhodamine 6G (Φ_f = 0.88 in ethanol) as standard. Time-resolved fluorescence decay measurements were carried out at the magic angle using a picosecond-diode-laser-based, time-correlated single-photon-counting (TCSPC) fluorescence spectrometer (IBH, UK). All the decays were fitted to a single exponential.

Field emission scanning electron microscopy (FE-SEM)

FE-SEM images were taken on a Jeol JSM IT-100 instrument. The accelerating voltage was set 10 kV and a probe current value of 30, under high vacuum mode. A long working distance was used to increase the depth of field and allow for tilting. The sample was adhered to the sample holder using colloidal graphite paint.

Atomic force microscopy (AFM)

The surface topography of hydrogels was investigated by atomic force microscopy with a Dimension 3100 AFM microscope controlled by a Nanoscope IIIa controller, (Digital Instruments, Santa Barbara, CA, USA). This was operated in tapping-mode, using standard silicon cantilevers (Budget Sensors, http://www.budgetsensors.com/) with a 7 nm tip-radius and a 42N.m^{-1} spring constant (nominal values). In summary, a thin slice of transparent swell hydrogel was cut manually from a mass of hydrogel with a stainless steel razor blade. A freshly cleaved 10 mm diameter disk of mica was applied to the cut surface of the hydrogel. After 15 min, the disk was peeled off the hydrogel surface and mounted in the AFM. Multiple images were examined and edited using WxSM software (Nanotec Electronica S.L, Madrid, Spain) to generate topography, phase and profile data.[16]

Rheology

The rheological experiments were performed on an Anton Paar MCR 301 rheometer. All the experiments were carried out at 25 °C using a 50 mm parallel plate with plate gap of 0.5 mm. The hydrogel was placed between the parallel plate and the platform with a solvent trap to avoid evaporation of water. A frequency of 1 Hz was used for the oscillatory strain sweep measurements while a constant strain amplitude of 1 % was used in the frequency sweeps.

Results and discussion

Preparation BDP-CS hydrogels

Water-soluble BODIPY-chitosan hydrogels were prepared by reacting chitosan with 3,5-diformyl-4,4-difluoro-4-bora-3a,4a-diaza-*s*-indacene at 25 °C within 30 min. This Schiff-base cross-linking between the amine group of chitosan and the formyl groups of BDP yields an interconnected 3D matrix linked through imine bonds, as shown in Figure 1.

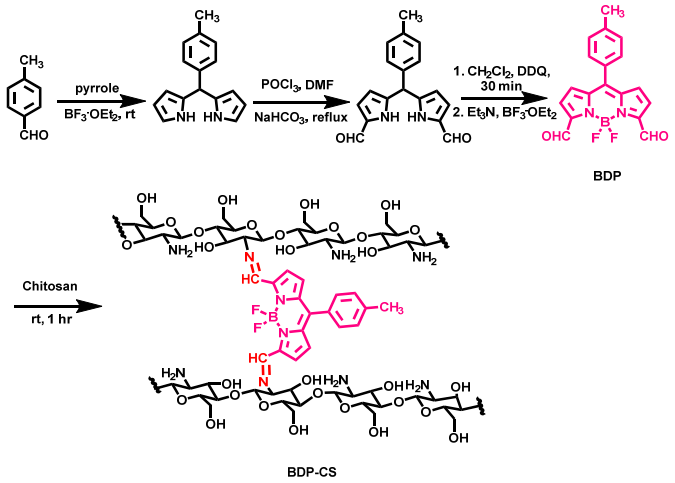

Figure 1. Synthesis of BDP and reaction with CS to yield BODIPY-chitosan (BDP-CS) hydrogels.

FT-IR spectra of 3,5-diformyl-BODIPY, chitosan and BDP-CS hydrogel are shown in Figure 2a. The absorption band at 1670 cm^{-1} was attributed to the asymmetric vibrations of the aldehyde group of BDP which completely disappeared in BDP-CS hydrogel spectrum. The FT-IR spectrum of BDP-CS hydrogel in comparison with the pure chitosan spectrum showed a characteristic absorption of the imine stretching vibration at 1629 cm^{-1} indicating the successful Schiff base cross-linking. Figure 2b shows the UV-vis spectrum of the BDP-CS hydrogel in aqueous media with the typical pattern of monomeric 3,5-diformyl-BODIPY in organic solvents with a strong absorption band at 528 nm and 559 nm. UV-vis spectra of BDP-CS hydrogels with different concentrations of BDP confirmed that there is no aggregation of the BODIPY units in water due to their covalent conjugation as a cross-linking gelator in the BDP-CS hydrogel.

To gain an insight into the morphologies of the BDP-CS hydrogel we used field-emission scanning electron microscopy (FE-SEM) and non-contact atomic force microscopy (AFM). For FE-SEM images, wet samples are not suitable under high vacuum conditions and thus the BDP-CS hydrogels were dehydrated by freeze drying. FE-SEM images of hydrogels samples with various total concentration of cross-linker are shown in Figure 3a-d and confirmed a three-dimensional porous morphology. The sponge-like microstructure is established by interconnected hollow spheres with diameters in the range of 80 µm and the holes are uniformly distributed over a large area. This structure is unique for using 3,5-diformyl-BODIPY as a bifunctional cross-linker in the hydrogel structure. The corresponding 3D structure exhibits large, open porosities that facilitate the entrance of water.

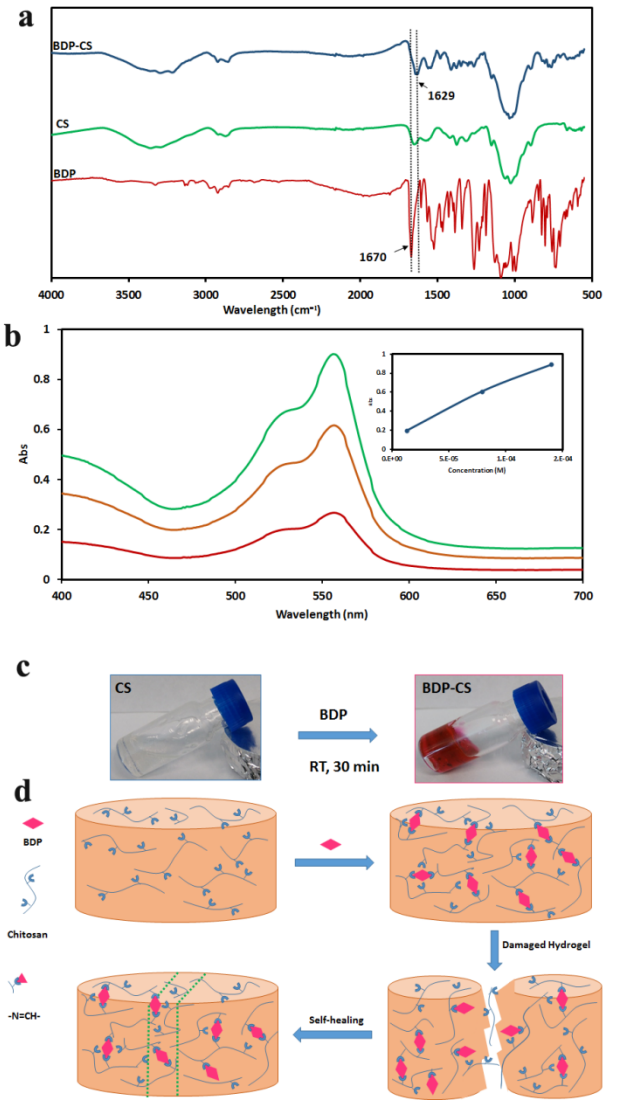

Figure 2. (a) FT-IR spectra of 3,5-diformyl-4,4-difluoro-4-bora-3a,4a-diaza-*s*-indacene (BDP), chitosan (CS) and BODIPY-chitosan hydrogel (BDP-CS). (b) Absorption spectra of BDP-CS hydrogels in H_2O at different concentrations of BDP 3.79×10^{-5} M, 2.5×10^{-5} M, 1.4×10^{-5} M in green, orange and red color, respectively. (c) Photograph of chitosan before gelation and BDP-CS hydrogel after gelation and irradiated by UV lamp. (d) Illustration showing the gelation and self-healing process.

The microstructure of the BDP-CS hydrogel could be affected by controlling the ratio of cross-linker to CS. The pore sizes at different concentrations of cross-linkers are summarized in Table 1. It can be clearly seen that the pore size decreases with increasing cross-linker concentration. In addition, the FE-SEM images displayed nano-layers on the pore surface of the hydrogel 3D network with a diameter from 100 to 400 nm (Figure S5, supplementary information (S.I.)).

AFM studies of BDP-CS hydrogels confirmed the formation of a 3D porous structure. AFM analysis is an effective method to provide surface topography and phase images. The AFM images of the BDP-CS hydrogel in Figure 3e,f show good agreement

Journal Name

ARTICLE

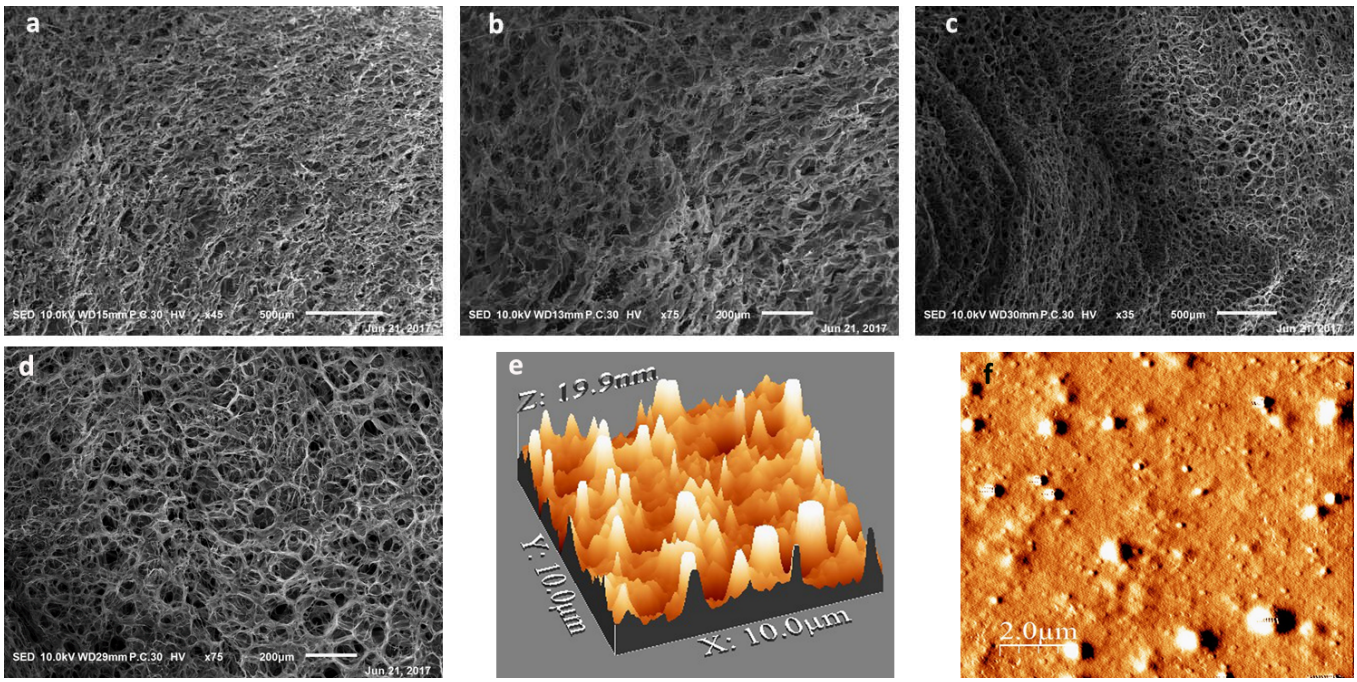

Figure 3. FE-SEM images of BDP-CS hydrogel at (a,b) 3 % w/w cross-linker, (c,d) 8 % w/w cross-linker at different magnifications, (e) AFM topographic (3D height), (f) AFM amplitude images of the BDP-CS hydrogel.

Table 1. Measured pore size and roughness of BDP-CS hydrogel by FE-SEM and AFM, respectively. Storage modulus measured with a rheometer at different concentrations of cross-linker.

Sample	Pore size (µm)	Roughness (Å)	G´ (pa)
Chitosan	-	2.32	-
BDP-CS 3 %	80	-	30
BDP-CS 5 %	-	25.32	90
BDP-CS 8 %	22	-	269

with the results of the FE-SEM studies. The pure chitosan and BDP-CS hydrogel were investigated in a comparative study. (Figure S7, S.I.) The AFM image in Figure 3f shows that the topography of the BDP-CS hydrogel is rough with a homogeneous distribution of porosity. The recorded roughness for BDP-CS hydrogel is 25.32 Å, which is higher than for the pure chitosan film (Table 1).

Rheological characterization and self-healing properties of BDP-CS hydrogels

To investigate the viscoelastic properties of the BDP-CS hydrogel a rheological analysis was carried out. The amount of energy stored in the sample is indicated by the storage modulus (G') and the amount of energy dissipated within the system under the oscillatory stress is shown by the loss modulus (G"). In order to survey the effect of different ratios of cross-linker on the mechanical properties of the BDP-CS hydrogel, rheological measurements were carried out for different concentrations of BDP in the hydrogel structure. Figure 4a shows the changes of G' as a function of frequency (ω) at 1.0 % strain, for 3, 5 and 8 % BDP-CS hydrogel, respectively. The values of G" versus frequency are shown in Figure 4b. The hydrogel state is revealed by the fact that the values of the storage modulus are higher than those of the loss modulus in all different samples. As expected, higher storage modulus values were obtained at higher percentages of cross-linked hydrogels. E.g., a 900 % increase in G' value (from 30 to 270 Pa) was observed upon increasing the concentration of BDP from 3 to 8 %. This improvement in mechanical strength is due to the interconnected 3D network of the hydrogel at high concentration of cross-linkers. Increasing the concentration of cross-linker in the BDP-CS hydrogel structure is a proven strategy for improving mechanical strength. The self-healing behavior of BDP-CS hydrogel was also investigated using rheology analysis of BDP-CS 3 % hydrogel which qualitatively showed the self-healing process (Figure 4c-d).

Journal Name

ARTICLE

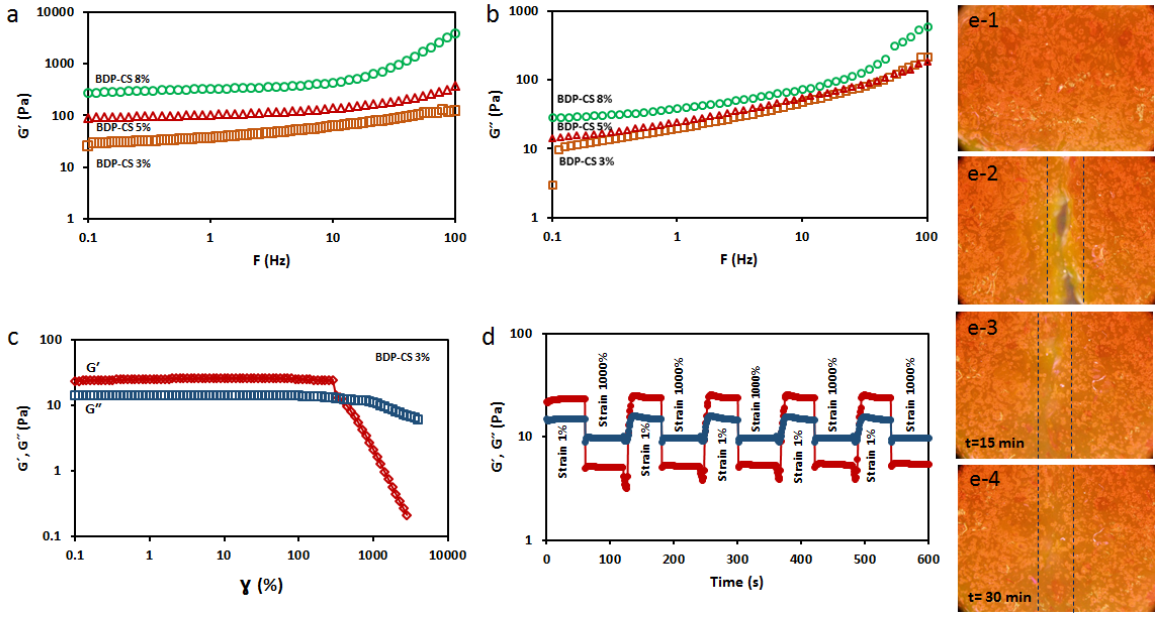

Figure 4. Rheology analysis of BDP-CS hydrogel. (a) Storage modulus (G') of different weight percentages of BDP as cross linkers in BDP-CS hydrogel at γ = 1.0 %. (b) Loss modulus (G") of different weight percentages of BDP cross linkers in BDP-CS hydrogel at γ = 1.0 %. (c) Storage modulus (G', red) and loss modulus (G", blue) of the BDP-CS hydrogel from strain amplitude sweep (strain 0.1 – 10000 %) at a fixed angular frequency of 1 Hz. (d) Recovery test for damage-healing properties of BDP-CS hydrogel 3 % at frequency of 1 Hz and alternating strain amplitudes of 1 % and 500 %. (e) Optical microscopy images of BDP-CS hydrogel: (e-1) original hydrogel, (e-2) hydrogel cut into two pieces, (e-3) after being self-healed for 15 min, (e-4) after self-healing for 30 min.

The elastic response of the BDP-CS hydrogel was analyzed by a strain amplitude sweep. At low strain, no significant changes in the values of G' and G" were observed. Figure 4c shows a decrease in the G' value above the yield strain region at γ about 355 %. The results of the strain amplitude sweep indicate that the storage modulus and loss modulus curves intersect at the strain about 355 %, indicating that the gel is between solid and fluid state near the critical point. The values of the storage modulus decrease upon increasing the strain to ~10,000 %, owing to the collapse of the gel networks. This can be attributed to the imine bonds breaking after being exposed to high shear strain.

Considering the results of the strain amplitude sweep, step strain measurements were carried out in order to study the recovery behavior of the BDP-CS hydrogel. As shown in Figure 4d the hydrogel was treated under low strain (γ = 1 %), which is below the onset of plastic deformation. The results show G' values are higher than G" in the hydrogel state. Upon increasing the strain to 500 %, the hydrogel loses its mechanical stability, which is confirmed by the inversion of G' and G" values, so that G" values are higher than G'. It was observed that the G' value intensity decreased from ~23 to 4 Pa and they are smaller than G", resulting in dissociation of Schiff base linkages.[1b] However, when high strain was discontinued and a low strain (γ = 1 %) was used, the G' values recovered to the main values and the hydrogel returned to the initial state, indicating the recovery of the cross-linked network. Similarly, when large strain (500 %) and a small strain (1 %) were alternatively applied, the G" values restored to the initial value. This self-recovery process was continued for eight cycles to establish the self-healing property.

The self-healing process of BDP-CS hydrogel was also investigated by optical microscopy (Fig. 4e). The images clearly verify the two separated hydrogel pieces could join to each other with rebuilding of the cross-linked gel network within 30 min.

This is further illustrated by the experiment shown in Figure 5. We tested the macroscopic self-healing behavior of the BDP-CS hydrogel by cutting the hydrogel into four pieces with different colors and after that, connecting them back to the original shape. Within 1 h at room temperature – without any external intervention – the hydrogel pieces connected together and solidified. Figure 5d,e shows the differently colored pieces integrated with each other, confirming efficient self-healing, i.e. reformation of imine bonds across the interface.

The rheology recovery test confirmed that the hydrogels behaved like liquid at high shear strain and recovered when the stress was removed. This indicates that BDP-CS hydrogels can be used as injectable gels. To confirm this, two differently colored BDP-CS hydrogels were loaded into a syringe (Fig. 5a,b). Figure 5a-b suggests that the hydrogel was injectable. After injecting into a vial, the extruded BDP-CS hydrogel came together to form an integrated piece due to its self-healing ability. The healed hydrogel piece maintained its shape when it was immersed in PBS (phosphate buffer saline, pH 7.0) at pH= 7.0 for 4 h (Fig. 5c). This reveals that the dynamic reaction (Schiff-base formation) between the amine groups of chitosan and aldehyde groups of 3,5-diformyl-BODIPY as the functional groups is crucial for the self-healing behavior.

In order to investigate the water/pH-stability of the hydrogel the BDP-CS-hydrogel was immersed in three different media: basic (aq. NaOH, 6 M), neutral (water, pH = 7) and acidic (aq. HCl, 6 M) and incubated at room temperature for 1 hour. The hydrogel showed good stability under basic conditions, was perfectly stable under neutral conditions, while in acidic solution it dissolved within 5 min (Figure S8).

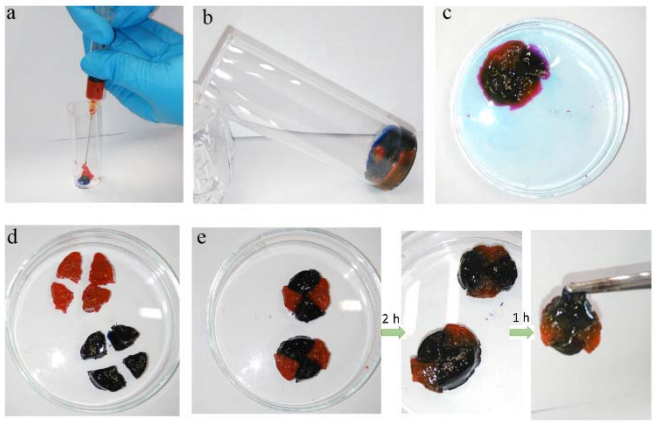

Figure 5. Photographs of the self-healing process and beam-shaped compression test of the BDP-CS hydrogel. (a) Two different colors of hydrogel (one with its native color and the other stained with methylene blue) injected in vial; (b) the hydrogels combined into one piece after 1 h; (c) immersed in PBS (pH 7.0) for 4 h, the healed hydrogel disk can retain its shape; (d) disk-shaped hydrogels were cut into 8 equal pieces, (e) the self-healed hydrogel disks can stand after healing for 3 h at 25 °C without any external intervention.

Photophysical and photochemical properties of BDP-CS hydrogels

BODIPY dyes are strongly UV-absorbing small molecules that emit relatively sharp fluorescence peaks with high quantum yields.[1] Small modifications to their structures enable tuning of their fluorescence characteristics; consequently, these dyes are widely used to label proteins and DNA.[17] The absorption and emission properties of the novel BDP-CS hydrogel was recorded in water and DMSO and are shown in Figure 6a-1,a-2 and summarized in Table 2. In water, the BDP-CS hydrogel showed a characteristic strong absorption band corresponding to a $S_0 \rightarrow S_1$ transition at 560 nm with one vibronic component on the higher energy side at 528 nm. In water the absorption bands of the BDP-CS hydrogel exhibited a bathochromic shift of ca. 20 nm in comparison to DMSO. The BDP-CS hydrogel showed a strong emission band at 575 nm in water which is bathochromically shifted by 24 nm compared to DMSO. The quantum yield was significantly improved to φ = 0.11 and 0.29 in water and DMSO, respectively. This reflects **a** 14.5 fold improvement in fluorescence quantum yield compared to the monomeric BDP[15] unit (φ = 0.02 in DMSO).

The emission spectra of the BDP-CS hydrogel at high and low concentrations of 3,5-diformyl-BODIPY in water are shown in Figure 6b. The main differences are that the fluorescence emission spectrum of the highly concentrated hydrogel is red-shifted and the fluorescence intensity decreases slightly compared to the low concentration one. This is mainly due to a reduction in the donor-acceptor separation at high concentration and hence the resonance energy transfer of the BODIPY dyes in the hydrogel network, which reduces the fluorescence intensity of the BODIPY units. However, the efficiency of energy transfer is mainly sensitive to the amount of separation between the donor and acceptor.[18] Figure 6c exhibits the absorption and emission spectra obtained from the highly concentrated and dilute BDP-CS hydrogel samples. There is a better spectral overlap between the fluorescence and absorption spectra of the concentrated BDP-CS hydrogel, compared to the dilute sample. This indicates that the underlying predominant fluorescence mechanism is based on the fluorescence resonance energy transfer (FRET).[10b]

Table 2. Spectroscopic characteristics of the BODIPY dye in the hydrogel network in different solvents.

Compound	solvent	λ_{abs} (nm) [a]	λ_{em} (nm) [a]	φ_{em}	τ (ns)	$K_r(10^9\ s^{-1})$	$K_{nr}(10^9\ s^{-1})$
BDP-CS hydrogel	H_2O	560	575	0.11	0.13	0.846	6.84
	DMSO	540	551	0.29	0.15	0.933	4.73
BDP[15]	DMSO	519	535	0.02	---	---	---

[a] Concentration of BDP in BDP-CS hydrogels for absorption and emission was 2.5×10^{-5} M in both H_2O and DMSO.

The fluorescence decay profiles of the BODIPY-hydrogel was determined with excitation at 540 nm (corresponding to the BODIPY unit) and was fitted to a single exponential and the singlet state lifetime(s) data is in agreement with the quantum yield data. 3,5-Diformyl-BODIPY has very weak fluorescence and the life-time was not fitted in the single exponential in DMSO (Table 2) indicating it has a very short life time in DMSO. In contrast, the BDP-CS hydrogel is strongly fluorescent and has longer fluorescence life times, both DMSO and water. The fluorescence lifetime (τ) is composed of two components, the radiative and non-radiative decay rates. Enhancement of fluorescence can be due to increased radiative recombination or a decrease in non-radiative recombination. In the BDP-CS hydrogel the fluorescence lifetimes were 0.13 and 0.15 ns in water and DMSO, respectively. As clearly shown from the data,

Journal Name

ARTICLE

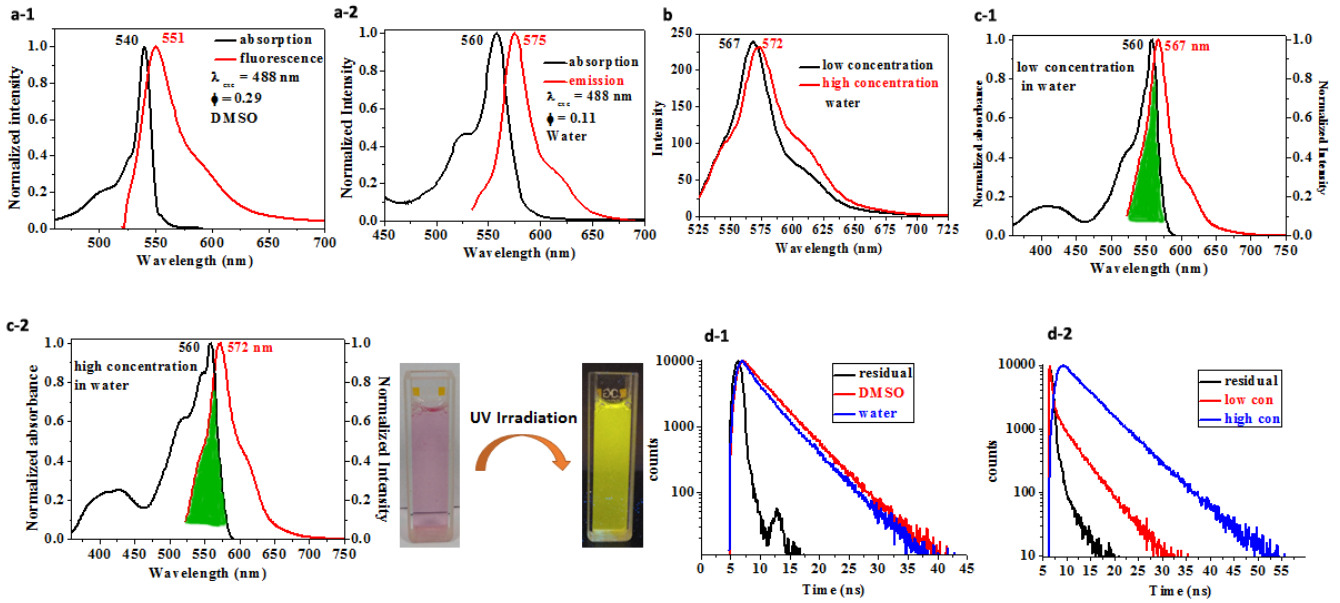

Figure 6. Normalized absorption and emission spectra of BDB-CS hydrogel (a-1) in DMSO (2.5×10^{-5} M) (a-2) in water (2.5×10^{-5} M); (b) fluorescence intensity of highly concentrated and low concentrated BDP-CS hydrogel in water; normalized absorption and emission spectra (c-1) at low concentrated (c-2) high concentrations of BDP in BDP-CS hydrogel in water; comparison of fluorescence decay profiles of BDP-CS hydrogel (d-1) in DMSO and H_2O, (d-2) at low (1.4×10^{-5} M) and high (3.79×10^{-5} M) concentrations of cross linker in water.

the radiative recombination was increased and the non-radiative recombination was decreased upon going from water to DMSO solvent (Table 2). In addition, the fluorescence life-time of BDP-CS hydrogels with different BODIPY concentrations were determined. At the higher concentration the life time was 0.13 ns and the lower concentration life time was 0.10 ns. Different concentrations induced a change in the life-time of the dyes (Fig. 6d-2). This is one more verification that the fluorescence dynamics does not obey self-quenching and conforms to a resonance energy transfer mechanism.[10b] The reasonable quantum yield and prolonged fluorescence lifetime in aqueous solution make the BDP-CS hydrogels an excellent tag for biological materials and also suitable as a new fluorescent probe.

Conclusions

In summary, we have developed a simple and effective way to prepare highly water-soluble neutral BODIPY formulations by cross-linking them in chitosan-based 3D hydrogel networks. This new fluorescent, self-healing, and injectable hydrogel was fabricated using a Schiff-based reaction. The dynamic nature of the hydrogel was confirmed by rheological recovery tests and macroscopic and microscopic self-healing tests. The fluorescence quantum yield of the new hydrogels was 14.5 times higher than that of the 3,5-diformyl-BODIPY monomer due to the absence of dye aggregation in the hydrogel 3D network, even at high concentrations of cross linker. In addition, the fluorescence life time of the BDP-CS hydrogel at different concentrations, verified that the fluorescence dynamics does not obey self-quenching and conforms to resonance energy transfer. This approach of creating fluorescent hydrogels using cross-linking BODIPY monomers with its attendant improvements in mechanical and photochemical properties and the acceptable values of fluorescent lifetimes creates opportunities for new optical polymer designs and uses for biomedical applications such as an implantable fluorescent hydrogels.

Acknowledgements

This work was supported by grants from Science Foundation Ireland (IvP 13/IA/1894) and the Research Council of Arak University, Iran.

Notes and references

1 (*a*) A. Treibs and F.-H. Kreuzer, Difluorboryl-Komplexe von Di- und Tripyrrylmethenen, *Liebigs Ann Chem.*, 1968, **718**, 208–223; (*b*) G. Ulrich, R. Ziessel and A. Harriman, The chemistry of fluorescent bodipy dyes: Versatility unsurpassed, *Angew. Chem. Int. Ed.*, 2008, **47**, 1184–1201; (*c*) A. Loudet and K. Burgess, BODIPY Dyes and Their Derivatives: Syntheses and Spectroscopic Properties, *Chem. Rev.*, 2007, **107**, 4891–4932.

2 (*a*) N. Boens, V. Leen and W. Dehaen, Fluorescent indicators based on BODIPY, *Chem. Soc. Rev.*, 2012, **41**, 1130–1172; (*b*) A. Kamkaew, S. H. Lim, H. B. Lee, L. V. Kiew, L. Y. Chung and K. Burgess, BODIPY dyes in photodynamic therapy, *Chem. Soc. Rev.*, 2013, **42**, 77–88; L. Yuan, W., K. Zheng, L. He and W. Huang, Far-red to near infrared analyte-responsive fluorescent probes based on organic fluorophore platforms for fluorescence imaging, *Chem. Soc. Rev.*, 2013, **42**, 622–661.

3 N. I. Georgiev, R. Bryaskova, T. Tzoneva, I. Ugrinova, C. Detrembleur, S. Miloshev, A. M. Asiri, A. H. Qusti and V. B. Bjinov, A novel pH sensitive water soluble fluorescent nanomicellar sensor for potential biomedical applications, *Bioorg. Med. Chem.*, 2013, **21**, 6292–6302.

4 (*a*) C. Li and S. Liu, Polymeric assemblies and nanoparticles with stimuli-responsive fluorescence emission characteristics, *Chem. Commun.*, 2012, **48**, 3262–3278; (*b*) A. Nagai, J. Miyake, K. Kokado, Y. Nagata and Y. Chujo, Highly luminescent BODIPY-based organoboron polymer exhibiting supramolecular self-assemble structure, *J. Am. Chem. Soc.*, 2008, **130**, 15276–15278.

5 (*a*) L. Li, J. Han, B. Nguyen and K. Burgess, Syntheses and Spectral Properties of Functionalized, Water-Soluble BODIPY Derivatives, *J. Org. Chem.*, 2008, **73**, 1963–1970; (*b*) T. Bura and R. Ziessel, Water-Soluble Phosphonate-Substituted BODIPY Derivatives with Tunable Emission Channels, *Org. Lett.*, 2011, **13**, 3072–3075; (c) K. Gießler, H. Griesser, D. Göhringer, T. Sabirov and C. Richert, Synthesis of 3′-BODIPY-labeled active esters of nucleotides and a chemical primer extension assay on beads, *Eur. J. Org. Chem*., **2010**, 3611–3620; (*d*) Ö. Dilek and S. L. Bane, Synthesis, spectroscopic properties and protein labeling of water soluble 3,5-disubstituted boron dipyrromethanes, *Bioorg. Med. Chem. Lett.*, 2009, **19**, 6911–6913; (*e*) S. C. Dodani, Q. He and C. J. Chang, A turn-on fluorescent sensor for detecting Nickel in living cells, *J. Am. Chem. Soc.*, 2009, **131**, 18020–18021; (*f*) S.-L. Niu, G. Ulrich, P. Retailleau, J. Harrowfield and R. Ziessel, New insights into the solubilization of Bodipy dyes, *Tetrahedron Lett.*, 2009, **50**, 3840–3844.

6 (*a*) S. Zhu, J. Zhang, G. Vegesna, F.-T. Luo, S. A. Green and H. Liu, Highly Water-Soluble Neutral BODIPY Dyes with Controllable Fluorescence Quantum Yields, *Org. Lett.*, 2011, **13**, 438–441; (*b*) S. Atilgan, T. Ozdemir and E. U. Akkaya, A Sensitive and Selective Ratiometric Near IR Fluorescent Probe for Zinc Ions Based on the Distyryl−Bodipy Fluorophore, *Org. Lett.*, 2008, **10**, 4065–4067; (*c*) V. H. Yen, L. Micouin, C. Ronet, G. Gachelin and M. Bonin, Total Enantioselective Synthesis and In Vivo Biological Evaluation of a Novel Fluorescent BODIPY *α*-Galactosylceramide, *ChemBioChem*, 2003, **4**, 27–33; (*d*) S. L. Niu, G. Ulrich, R. Ziessel, A. Kiss, P.-Y Renard and A. Romieu, Water-Soluble BODIPY Derivatives, *Org. Lett.*, 2009, **11**, 2049–2052; (*e*) R. París, I. Quijada-Garrido, O. García and M. Liras, BODIPY-Conjugated Thermo-Sensitive Fluorescent Polymers Based On 2-(2-methoxyethoxy)ethyl methacrylate, *Macromolecules*, 2011, **44**, 80–86.

7 (*a*) N. A. Peppas, J. Z. Hilt, A. Khademhosseini and R. Langer, Hydrogels in Biology and Medicine: From Molecular Principles to Bionanotechnology, *Adv. Mater.*, 2006, **18**, 1345–1360; (*b*) E. Caló and V. V. Khutoryanskiy, Biomedical applications of hydrogels: A review of patents and commercial products, *Eur. Polym. J.*, 2015, **65**, 252–267.

8 (*a*) S. Belali, A. R. Karimi and M. Hadizadeh, Novel nanostructured smart, photodynamic hydrogels based on poly(N-isopropylacrylamide) bearing porphyrin units in their crosslink chains: a potential sentesizer sustem in cancer therapy, *Polymer*, 2017, **109**, 93–105; (*b*) A. R. Karimi, A. Khodadadi and M. Hadizadeh, A nanoporous photosensitizing hydrogel based on chitosan cross-linked by zinc phthalocyanine: an injectable and pH-stimuli responsive system for effective cancer therapy, *RSC Adv.*, 2016, **6**, 91445–91452.

9 (*a*) I. Lynch and K. A. Dawson, Release of Model Compounds from “Plum-Pudding”-Type Gels Composed of Microgel Particles Randomly Dispersed in a Gel Matrix, *J. Phys. Chem. B*, 2004, **108**, 10893–10898; (*b*) M. Hecht, W. Kraus and K. Rurack, A highly fluorescent pH sensing membrane for the alkaline pH range incorporating a BODIPY dye, *Analyst*, 2013, **138**, 325–332; (*c*) Y. Zhang, S. Swaminathan, S. C. Tang, J. Garcia-Amoros, M. Boulina, B. Captain, J. D. Baker and F. M. Raymo, Photoactivatable BODIPYs Designed To Monitor the Dynamics of Supramolecular Nanocarriers, *J. Am. Chem. Soc.*, 2015, **137**, 4709–4719; (*d*) B. J. Müller, S. M. Borisov and I. Klimant, Red- to NIT-Emitting, BODIPY-Based, K^+-Selective Fluoroionophores and Sensing Materials, *Adv. Funct. Mater.*, 2016, **26**, 7697–7707; (*e*) B. J. Müller, T. Rappitsch, C. Staudinger, C. Ruschitz, S. M. Borisov and I. Klimant, Sodium-Selective Fluoroionophore-Based Optodes for Seawater Salinity Measurement, *Anal. Chem.*, 2017, **89**, 7195–7202.

10 (*a*) S.-H. Lee, J. J. Moon, J. S. Miller and J. L. West, Poly(ethylene glycol) hydrogels conjugated with a collagenase-sensitive fluorogenic substrate to visualize collagenase activity during three-dimensional cell migration, *Biomaterials*, 2007, **28**, 3163–3170; (*b*) S. Acikgoz, G. Aktas, M. N. Inci, H. Altin and A. Sanyal, FRET between BODIPY Azide Dye Clusters within PEG-Based Hydrogel: A Handle to Measure Stimuli Responsiveness, *J. Phys. Chem. B*, 2010, **114**, 10954–10960.

11 P. B. Malafaya, G. A. Silva and R. L. Reis, Natural-origin polymers as carriers and scaffolds for biomolecules and cell delivery in tissue engineering applications, *Adv. Drug Del. Rev.*, 2007, **59**, 207–233.

12 N. Bhattarai, J. Gunn and M. Zhang, Chitosan-based hydrogels for controlled, localized drug delivery, *Adv. Drug. Del. Rev.*, 2010, **62**, 83–99.

13 M. N. Kumar, R. A. Muzzarelli, C. Muzarelli, H. Sashiwa and A. J. Domb, Chitosan chemistry and pharmaceutical perspectives, *Chem. Rev.*, 2004, **104**, 6017–6084.

14 B. Yang, Y. Zhang, X. Zhang, L. Tao, S. Li and Y. Wei, Facilely prepared inexpensive and biocompatible self-healing hydrogel: a new injectable cell therapy carrier, *Polym. Chem.*, 2012, **3**, 3235–3238.

15 S. Madhu, M. R. Rao, M. S. Shaikh and M. Ravikanth, 3.5-Diformylboron dipyrromethenes as flurescent pH sensors, *Inorg. Chem.*, 2011, **50**, 4392–4400.

16. Horcas I, Fernandez R, Gomez-Rodriguez JM, Colchero J, Gomez-Herrero J, Baro AM. 2007. WSXM: A software for scanning probe microscopy and a tool for nanotechnology. *Rev. Scient. Instrum.*, 2007, **78**, 013705-013708.

17 (*a*) G. MacBeath and S. L. Schreiber, Printing Proteins as Microarrays for High-Throughput Function Determination, *Science*, 2000, **289**, 1760–1763; (*b*) S. Kurata, T. Kanagawa, K. Yamada, M. Torimura, T. Yokomaku, Y. Kamagata and R. Kurane, Fluorescent quenching-based quantitative detection of specific DNA/RNA using a BODIPY (R) FL-labeled probe or primer, *Nucleic Acids Res.*, 2001, **29**, e34.

18 S. A. E. Marras, F. R. Kramer and S. Tyagi, Efficiencies of fluorescence resonance energy transfer and contact-

mediated quenching in oligonucleotide probes, *Nucl. Acids Res.*, 2002, **30**, e122.

ToC graphic